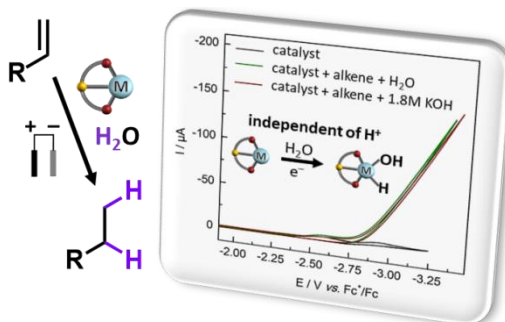


# Proton Independent Electrocatalytic Transfer Hydrogenation of Styrene with $[(^t\text{BuPCP})\text{Ir}(\text{H})(\text{Cl})]$ and Water

Patrick Mollik, Alexander M. Frantz, Dominik P. Halter \*

Department of Chemistry, Technical University of Munich, Lichtenbergstraße 4, 85787 Garching, Germany.

**ABSTRACT:** A new pathway of electrocatalytic transfer hydrogenation with neutral water as the H-donor was discovered using  $[(^t\text{BuPCP})\text{Ir}(\text{H})(\text{Cl})]$  (**1**) as the catalyst and styrene as a model substrate in THF electrolyte. Cyclic voltammetry experiments with **1** revealed that two subsequent reductions at  $-2.55$  and  $-2.84$  V vs.  $\text{Fc}^+/\text{Fc}$  trigger the elimination of  $\text{Cl}^-$  and afford the highly reactive anionic Ir(I) hydride complex  $[(^t\text{BuPCP})\text{Ir}(\text{H})]^-$  (**2**). The identity of **2** and its reactivity were further investigated by LIFDI-MS, which confirmed **2** as reactive species in the alkene hydrogenation cycle. Bulk electrolysis and chronoamperometry for electro-hydrogenation of styrene established ethylbenzene as the only product, formed with high faradaic efficiency of 96% and a turnover frequency of  $1670\text{ h}^{-1}$  at an electrolysis potential of  $-3.1$  V, with insignificant  $\text{H}_2$  formation. Importantly, the electro-hydrogenation performance of **1** remained constant upon addition of KOH to the electrolyte, which suggests a reaction mechanism that is independent of free  $\text{H}^+$ . Instead, the reactive Ir-hydrides are regenerated by oxidative addition of  $\text{H}_2\text{O}$  to the complex, which creates a reaction cascade that is reminiscent of metal-hydride formation in classical transfer hydrogenation systems. As such, the herein presented study on electrocatalytic transfer hydrogenation (e-TH) with  $\text{H}_2\text{O}$  as the H-donor is different from the plethora of other electro-hydrogenation studies that operate *via*  $\text{H}^+$  reduction, often in low-pH electrolyte. These findings may inspire the general, pH independent use of  $\text{H}_2\text{O}$  as H-donor in conjunction with electrochemistry, to replace isopropanol or formate as intrinsically reducing H-donors in the many existing examples of classical transfer hydrogenation.



## INTRODUCTION

Hydrogenation of organic molecules is a process of paramount importance for the synthesis of base- and fine chemicals, pharmaceutically active compounds, and energy carriers, as well as for biomass valorization, both on industrial and laboratory scale.<sup>1–7</sup> To avoid challenges of handling gaseous  $\text{H}_2$  at high temperatures and pressures necessary for chemical hydrogenation (CH), transfer hydrogenation (TH) has matured as a powerful alternative.<sup>1,8,9</sup> TH employs chemical H-donors such as predominantly used isopropanol or formic acid as a substitute for  $\text{H}_2$ . In both cases of CH and TH, the reduction equivalents for the net reduction of substrates during hydrogenation are provided by  $\text{H}_2$  or the H-donor as chemical reducing agents, respectively.

For increased atom economy and cost efficiency, it would be desirable to enable  $\text{H}_2\text{O}$  as a cheap and abundant H-donor for TH instead of isopropanol or formate.<sup>10</sup> However,  $\text{H}_2\text{O}$  cannot provide the necessary reduction equivalents, which is why existing examples of hydrogenation with  $\text{H}_2\text{O}$  depend on the use of external reducing agents including Zn powder,<sup>10–12</sup> In powder,<sup>13</sup> or bis(pinacolato)diboron.<sup>14,15</sup> Electrochemistry can be an elegant substitute for such sacrificial electron donors,

which has led to a third branch of hydrogenation catalysis, namely electrocatalytic hydrogenation (ECH). Remarkable examples of ECH have been reported for the conversion of alkenes to alkanes,<sup>16,17</sup> selective semi-hydrogenation of alkynes to alkenes,<sup>18,19</sup> exhaustive hydrogenation of arenes,<sup>20–22</sup> selective hydrogenation of arenes to 1,4-dienes,<sup>23</sup> hydrogenation of organic carbonyls,<sup>24,25</sup> or the de-oxygenation of biomass.<sup>26–28</sup> ECH has even proven to be a powerful method for the synthesis of selectively deuterated alkenes.<sup>29</sup> Both, noble metal electrodes and molecular catalysts are employed for these conversions.<sup>30</sup> The dominant common aspect of all these examples is that they rely on  $\text{H}^+$  reduction, often in highly acidic electrolyte. The working principle is to either generate  $\text{H}_2$  or surface hydrides *in situ* at the electrode for immediate consumption by a coupled hydrogenation reaction.<sup>31</sup> Examples of molecular ECH catalysts likewise operate by formation of reactive metal-hydride species *via*  $\text{H}^+$  reduction, with a remarkable exception by Peters and coworkers, who elegantly separated redox reactive metal center and proton acceptor site in their anilinium cobaltocene catalyst.<sup>25</sup> While these existing systems succeed at avoiding external  $\text{H}_2$  gas feeds or sacrificial electron donors for hydrogenation, several drawbacks impede application. In many cases faradaic efficiencies for hydrogenated products are low,

given that H<sub>2</sub> evolution (HER) remains the dominant process.<sup>32</sup> Also poor solubility of most relevant organic substrates in acidic aqueous electrolytes requires less convenient emulsion electrolysis with the use of surfactants.<sup>33,34</sup> The requirement of high proton activity may interfere with functional groups of substrates that cannot tolerate low pH, and the harsh conditions of acidic electrolyte can lead to side reactions. Exemplarily, for ECH of toluene to methylcyclohexane on Pt electrodes in acid electrolyte, side reactions as severe as C–C bond cleavage to yield CH<sub>4</sub> and cyclohexane were observed.<sup>33</sup> Finally and importantly, with H<sub>2</sub>O oxidation (OER) at the counter electrode, low pH electrolytes cause high overpotentials, catalyst degradation, and sluggish kinetics of the coupled oxidation reaction.<sup>35</sup> This generates a high cell potential and limits overall achievable process efficiencies. For the multitude of these reasons, it would be desirable to establish ECH reactions that proceed in organic electrolyte with neutral pH water, or even in alkaline media, instead of under acidic conditions.

Drawing from extensive literature on TH,<sup>1,8</sup> and inspired by examples that show metal-hydrides can also be formed by oxidative addition of H<sub>2</sub>O to low-valent transition metal complexes instead of by H<sup>+</sup> reduction,<sup>36</sup> we hypothesized that a proton independent pathway of electrocatalytic transfer hydrogenation (e-TH) should be accessible. For the herein presented proof of principle study, the electrochemically accessible redox reactivity of the Ir(III) pincer complex [(<sup>t</sup>BuPCP)Ir(H)(Cl)] (**1**) and electrochemically triggered chemical reactions were investigated. The e-TH performance of **1** was monitored upon addition of H<sub>2</sub>O as the H-donor under neutral and alkaline conditions, with styrene as a model substrate in organic electrolyte. Successful production of ethylbenzene indeed suggested independence of H<sup>+</sup> activity in the electrolyte. Mechanistic studies and stoichiometric control reactions revealed that the e-TH at room temperature proceeds *via* an EC mechanism, in which a fleeting anionic Ir(I) hydride complex is electro-generated as the key reactive species. The combined results suggest that the iridium hydride is regenerated by oxidative addition of water in reminiscence of classical transfer hydrogenation. This represents a major difference compared to existing electro-hydrogenation catalysts that are principally driven by *in situ* proton reduction, and may inspire the general development of such e-TH reactivity.

## RESULTS AND DISCUSSION

[(<sup>t</sup>BuPCP)Ir(H)(Cl)] (**1**, with <sup>t</sup>BuPCP–H = 1,3-bis((di-tert-butylphosphino)methyl)benzene)<sup>37,38</sup> was synthesized according to literature procedures,<sup>37,38</sup> and studied by cyclic voltammetry (CV) to elucidate its ECH reactivity. At first, a CV of **1** was recorded in organic electrolyte (0.1 M Bu<sub>4</sub>NPF<sub>6</sub> (tetrabutylammonium hexafluorophosphate) in THF, all potentials referenced vs. Fc<sup>+</sup>/Fc) to reveal fundamental redox reactivity of the complex (Figure 1). In the examined potential window between +0.3 and –3.3 V (SI, Figure S1),

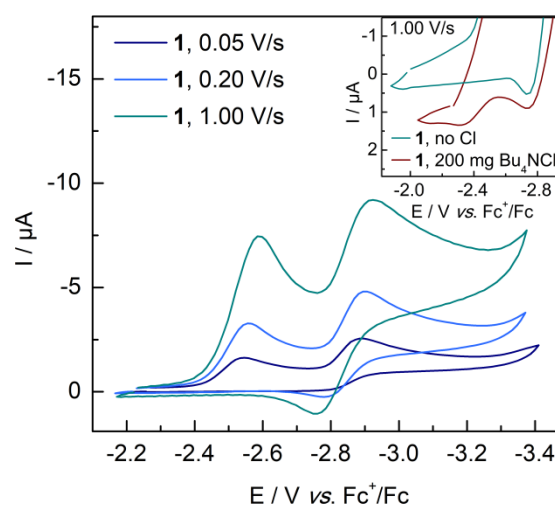


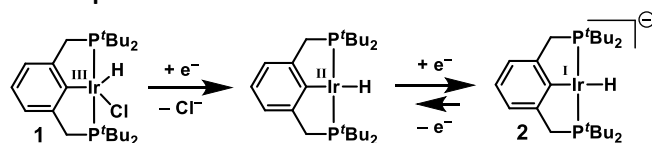
**Figure 1.** CV of **1** (4 mg) in THF with Bu<sub>4</sub>NPF<sub>6</sub> (350 mg in 3 mL) recorded at scan rates between 0.05 and 1 V/s using a GC disc (1 mm) working electrode, a Pt wire counter electrode, and a silver wire pseudo reference electrode. Inset: Control experiment showing that upon addition of 200 mg of Bu<sub>4</sub>NCl to the electrolyte solution, also the first reduction event becomes quasi reversible.

**1** features an irreversible reduction at a peak potential of –2.55 V, and a second reduction event at a half wave potential of –2.84 V, which shows quasi-reversibility at scan rates above 0.1 V/s (Figure 1). The first reduction event is assigned to an Ir(III)/Ir(II) reduction, which generates a fleeting anionic Ir(II) complex that instantly seeks charge neutrality by eliminating a Cl<sup>–</sup> ligand to yield the proposed intermediate Ir(II) species [(<sup>t</sup>BuPCP)Ir(H)]. This hypothesis is supported by the fact that the addition of chloride ions to the electrolyte in form of excess Bu<sub>4</sub>NCl (tetrabutylammonium chloride) renders the reduction at –2.55 V also quasi reversible at high scan rates (inset Figure 1 and SI, Figure S2), as Cl<sup>–</sup> dissociation from the reduced Ir complex is hampered (or re-coordination of Cl<sup>–</sup> is favored) in media with high chloride activity.

The second reduction event at –2.84 V is ascribed to an Ir(II)/Ir(I) couple, in which the proposed Ir(II) complex [(<sup>t</sup>BuPCP)Ir(H)] is reduced by another electron. At scan rates below 0.1 V/s, this reduction event is also irreversible, likely because of the well-known high reactivity of Ir(I) complexes that even activate C–H bonds of alkanes.<sup>39</sup> However, the fact that at higher scan rates the second reduction event becomes more and more reversible (see Figure 1), strongly suggests that the Ir(I) complex formed remains an anionic species [(<sup>t</sup>BuPCP)Ir(H)]<sup>–</sup> (**2**) that does not lose its hydride ligand. In fact, based on quantum chemical calculations by Ahlquist *et al.* an anionic hydride species related to **2**, but in a (<sup>t</sup>BuPOCOP)<sup>–</sup> pincer ligand environment, was previously proposed as the active species for electrochemical CO<sub>2</sub> reduction to formate with the POCOP analogue of complex **1**.<sup>40,41</sup> Further experimental evidence for the existence of such previously only theoretically proposed anionic Ir(I) hydrides like **2**, is now provided by

negative mode LIFDI-MS data (liquid injection field desorption/ionization mass spectrometry) obtained from *in situ* reduced solutions of **1** that were treated with electride solutions of  $[K(2.2.2\text{-cryptand})]^+$  as a source of solvated electrons (SI, section 2 for details).<sup>42</sup> Indeed, a prominent molecular ion peak at 587.25 m/z with the expected isotope pattern was observed as experimental evidence for the formation of **2** upon chemical two-electron reduction of **1** (SI, Figure S16). Accordingly, the electrochemical response of **1** presented in Figure 1 is interpreted as shown in Scheme 1.

**Scheme 1. Proposed Underlying Reactivity of the two Consecutive Electrochemical Reduction Events Observed for Complex 1.**



Curious to explore the chemical reactivity of the electrochemically produced anionic Ir(I) hydride **2**, we investigated the electrocatalytic hydrogenation of styrene as a model alkene with water as the H-donor. In analogy to quantum chemical calculations by Ahlquist *et al.* who predict CO<sub>2</sub> insertion into Ir–H bonds of anionic hydrides such as **2**, a direct activation of alkenes *via* formation of Ir(I)-alkyls could occur.<sup>40</sup> Alternatively, according to Jensen *et al.* Ir(I) ions in (<sup>t</sup>BuPCP)<sup>−</sup> ligand environment can undergo oxidative addition of H<sub>2</sub>O to form a reactive hydroxo-hydrido species.<sup>43</sup> For **2**, the oxidative addition of water

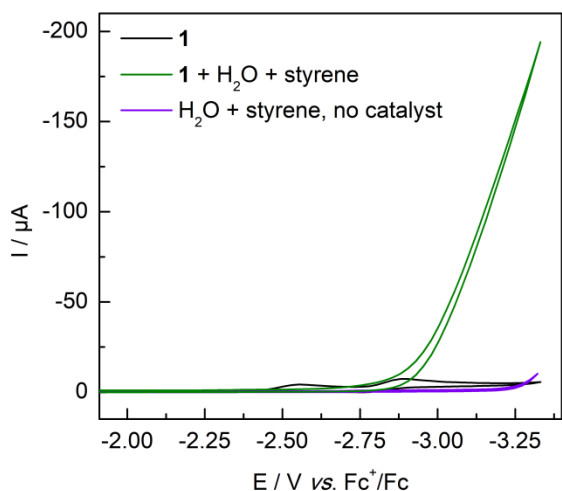


**Figure 2.** CV of **1** (4 mg) in THF with Bu<sub>4</sub>NPF<sub>6</sub> (350 mg in 3 mL) recorded at a scan rate of 0.2 V/s using a GC disc (1 mm) working electrode, a Pt wire counter electrode, and a silver wire pseudo reference electrode (black trace). The green trace shows the catalytic current response after addition of 100 μL degassed H<sub>2</sub>O and 100 μL styrene. The purple trace shows the CV response of the identical electrolyte solution with H<sub>2</sub>O and styrene, but in absence of catalyst **1**.

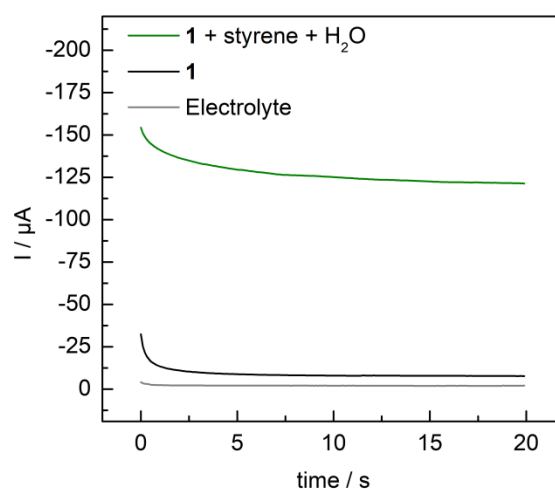


**Figure 3.** Chronoamperometry data obtained at an applied potential of −3.1 V for the electrolyte (3.00 mL of 0.1 M Bu<sub>4</sub>NPF<sub>6</sub> in THF with 100 μL of H<sub>2</sub>O) (grey), after addition of 3 mg **1** (black), and after addition of 100 μL styrene (green) to reach catalytic conditions.

would yield the fleeting anionic Ir(III) complex  $[(^t\text{BuPCP})\text{Ir}(\text{H})_2(\text{OH})]^-$ , proposed to spontaneously decay into charge neutral complex  $[(^t\text{BuPCP})\text{Ir}(\text{H})_2]$ ,<sup>40</sup> a well-known species active for alkene hydrogenation.<sup>44</sup> Besides activation of H<sub>2</sub>O molecules, the reduction of free H<sup>+</sup>, as in classical ECH, could occur as an alternative pathway to form the dihydride complex  $[(^t\text{BuPCP})\text{Ir}(\text{H})_2]$  from anionic **2**.<sup>45,46</sup> Accordingly, multiple reaction cascades for alkene hydrogenation can be envisioned with **2** as the active species and water as the H-donor. To evaluate the actual ECH reactivity of **1** and associated reactive species, we herein provide experimental characterization along with mechanistic consideration for the different possible reaction pathways.

Cyclic voltammetry experiments with catalyst precursor **1**, styrene, and water as the H-donor indeed yielded a strong catalytic current, visibly tied to the Ir(II)/Ir(I) reduction potential (Figure 2). Control experiments with either of the three components alkene, H<sub>2</sub>O or catalyst missing did not yield a comparable catalytic current response (SI, Figure S3). Most importantly, the simple addition of water to complex **1** did also not facilitate catalytic water reduction to produce H<sub>2</sub>, as evidenced by the lack of a catalytic current response in CV (SI, Figure S3), and no significant amount of H<sub>2</sub> being detected in GC-RGD headspace analysis (gas chromatograph with reducing gas detector) after bulk electrolysis experiments (SI, Figures S4 and S21). The desirable lack of competing H<sub>2</sub> evolution is likely due to the literature known water stability of iridium hydride functionalities.<sup>43,45,47</sup> Bulk electrolysis experiments performed at −3.1 V vs. Fc<sup>+</sup>/Fc in the presence of styrene, H<sub>2</sub>O, and catalyst precursor **1** revealed the formation of ethylbenzene as the hydrogenated product of styrene at high faradaic efficiency of 96% with a TON of 93, based on

$^1\text{H}$  NMR analysis of the electrolyte solution after electrolysis (SI, Figures S5 and S10).

A turnover frequency (TOF) of  $1670\text{ h}^{-1}$ , was determined for the hydrogenation of styrene with **1**, based on chronoamperometry experiments at  $-3.1\text{ V}$  following a protocol reported by Stahl and Rafiee (Figure 3 and eq. 1).<sup>48</sup>

$$\text{TOF} = \frac{[(Q_{\text{cat}} - Q_1) \times FE] \times 3600}{(Q_1 - Q_e) \times n \times t} \quad (1)$$

In eq. (1),  $Q_{\text{cat}}$  corresponds to the charge passed under catalytic conditions,  $Q_1$  corresponds to the charge passed in the presence of catalyst **1** without substrate,  $Q_e$  corresponds to the charge passed for the blank electrolyte solution.  $FE$  is the faradaic efficiency as determined by bulk electrolysis (*vide supra*),  $n$  is the number of electrons transferred to produce one molecule of product (here: ethylbenzene,  $n = 2$ ), and  $t$  is the time over which the charges were passed. Respective charges were determined by integrating over the experimental electrolysis currents as shown in Figure 3, excluding all charges passed during the first second, in order to eliminate capacitive current effects.

Together, the high selectivity and faradaic efficiency confirmed the excellent performance of catalyst **1** for electro-hydrogenation, which prompted us to further investigate the underlying catalytic reactivity.

**Mechanistic Considerations.** In order to understand the electrocatalyst's working principle, stoichiometric control reactions were performed. Based on the combined results (*vide infra*) and quantum chemical support published for  $\text{CO}_2$  reduction on the related POCOP system,<sup>40,45,46</sup> the reaction cascade shown in Scheme 2 is proposed as a likely mode of operation for the electro-hydrogenation of alkenes with complex **1**.

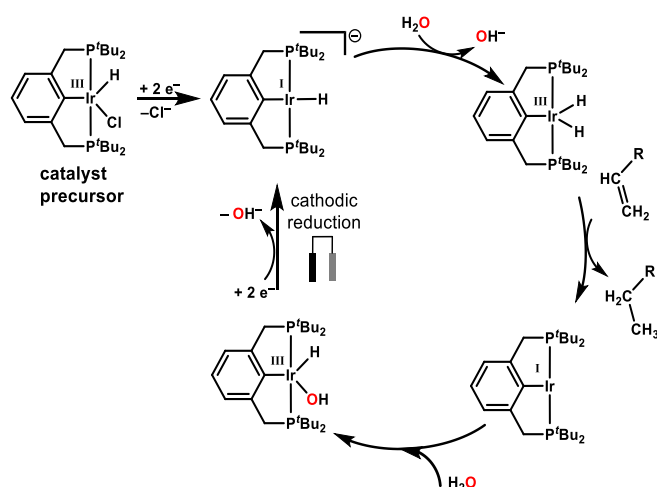
As already elucidated from CV analysis (*vide supra*), precatalyst **1** is converted into its active form **2**, by electrochemical reduction. Subsequently, **2** can either react

with an alkene to form an anionic Ir(I) alkyl species, in analogy to quantum chemical calculations for  $\text{CO}_2$  insertion,<sup>40,45</sup> or **2** could react with  $\text{H}_2\text{O}$  to yield charge neutral Ir(III) dihydride complex  $[(^t\text{BuPCP})\text{Ir}(\text{H})_2]$  under elimination of  $\text{OH}^-$ . In order to experimentally assess the feasibility of both pathways, solutions of Ir(III) complex **1** were again reduced chemically by addition of approximately two equivalents of solvated electrons in form of  $[\text{K}(2.2.2\text{-cryptand})]^+$  electrified solution (SI, section 2 for details). The *in situ* generated Ir(I) species was quenched by addition of  $\text{H}_2\text{O}$ , and subsequently analyzed by  $^1\text{H}$  NMR (SI, Figure S13) and LIFDI-MS (SI, Figure S18), to gain experimental insight into underlying reaction cascades of ECH with **1**. Quenching *in situ* generated **2** in  $\text{THF-d}_8$  by addition of  $\text{H}_2\text{O}$  afforded the distinctive hydride signals of Ir(III)-dihydride complex  $[(^t\text{BuPCP})\text{Ir}(\text{H})_2]$  at  $-19.53\text{ ppm}$ ,<sup>49</sup> as predicted by quantum chemical calculations,<sup>40,45,46</sup> together with unidentifiable decay products of highly reactive species **2** (SI, Figure S13). While the hydrogenation of alkenes by  $[(^t\text{BuPCP})\text{Ir}(\text{H})_2]$ , as shown in Scheme 2 is well documented,<sup>1</sup> two reaction pathways were previously discussed for its formation from anionic Ir(I) hydrides like **2**; namely the oxidative addition of  $\text{H}_2\text{O}$  with subsequent elimination of  $\text{OH}^-$  from the anionic species  $[(^t\text{BuPCP})\text{Ir}(\text{H})_2(\text{OH})]^-$ , or reductive O–H bond cleavage by **2** from coordinated  $\text{H}_2\text{O}$  under  $\text{OH}^-$  elimination.

For related Ir–POCOP complexes in acetonitrile, calculations by Ahlquist *et al.* yielded an activation barrier for reductive O–H bond cleavage that is energetically favored by *ca.*  $36\text{ kcal mol}^{-1}$  compared to classical oxidative addition of  $\text{H}_2\text{O}$ ; thus, rendering oxidative addition unlikely according to the transition state they found.<sup>40</sup> However, the anionic intermediate species analogous to  $[(^t\text{BuPCP})\text{Ir}(\text{H})_2(\text{OH})]^-$  that oxidative addition of  $\text{H}_2\text{O}$  to **2** would afford, was calculated at merely  $2.4\text{ kcal mol}^{-1}$  higher energy than the transition state for reductive O–H bond cleavage. Utilizing our new preparative protocol for *in situ* synthesis of **2** and subsequent characterization of short-lived species by negative mode LIFDI-MS, we therefore investigated the potential formation of  $[(^t\text{BuPCP})\text{Ir}(\text{H})_2(\text{OH})]^-$  experimentally.

Interestingly, quenching samples of **2** with  $\text{H}_2\text{O}$  generated a molecular ion peak at  $603.25\text{ m/z}$ , with a matching isotope pattern for the species  $[(^t\text{BuPCP})\text{Ir}(\text{OH})]^-$  (Figure S18) as a potential fragment of  $[(^t\text{BuPCP})\text{Ir}(\text{H})_2(\text{OH})]^-$  that forms upon  $\text{H}_2$  elimination. This possibility is supported by LIFDI-MS control experiments with independently synthesized tetrahydride species  $[(^t\text{BuPCP})\text{Ir}(\text{H})_4]$  (**3**), for which  $\text{H}_2$  elimination was also observed, due to high vacuum and high temperatures on the LIFDI instrument's emitter (SI, Figure S19). Alternative formation of  $[(^t\text{BuPCP})\text{Ir}(\text{OH})]^-$  via simple protonation of the hydride functionality in **2** to release  $\text{H}_2$  with exchange of the hydride ligand for  $\text{OH}^-$  could explain the LIFDI-MS result. This pathway, however, is not supported by  $^1\text{H}$  NMR reaction control performed in sealed J-Young NMR tubes, which did not show any  $\text{H}_2$  formation. Hence, we consider oxidative addition of  $\text{H}_2\text{O}$

**Scheme 2. Proposed Reaction Cascade for Electrocatalytic Hydrogenation of Styrene with Water.**





to complex **2** plausible under our experimental conditions, likely in parallel to the widely accepted reductive O–H bond cleavage pathway to form Ir(III) dihydride  $[(^t\text{BuPCP})\text{Ir}(\text{H})_2]$ .

Upon formation of  $[(^t\text{BuPCP})\text{Ir}(\text{H})_2]$ , the hydrogenation cycle is proposed to follow the classical established pathway for hydrogenation of non-polar substrates by redox reactive metal catalysts,<sup>1</sup> which yields the Ir(I) complex  $[(^t\text{BuPCP})\text{Ir}]$  as the next intermediate.  $[(^t\text{BuPCP})\text{Ir}]$  is known to undergo oxidative addition of  $\text{H}_2\text{O}$ ,<sup>40,43</sup> which replenishes the metal-hydride functionality *via* formation of  $[(^t\text{BuPCP})\text{Ir}(\text{H})(\text{OH})]$ . Ahlquist and coworkers suggest that this formal oxidative addition of  $\text{H}_2\text{O}$  to Ir(I) proceeds through an Ir(I)-aquo intermediate  $[(^t\text{BuPCP})\text{Ir}(\text{H}_2\text{O})]$ ,<sup>40</sup> from which hydride formation occurs *via* proton relay across a water cluster around the Ir center. A two-electron electrochemical reduction of the Ir(III) hydroxo hydrido complex then regenerates the reactive Ir(I) hydride **2**, to close the catalytic cycle.

It was previously proposed that for  $\text{CO}_2$  reduction with Ir pincer complexes, an alternative mechanism could exist in which  $\text{CO}_2$  inserts into the Ir–H bond of anionic Ir(I) hydride like **2**, to form the C–H bond of formate.<sup>40,45</sup> In context of the herein presented ECH of styrene this implies the possibility for an alternative catalytic cycle, in which styrene inserts into the Ir–H bond of **2**. Investigating this possibility, LIFDI-MS quenching experiments were again employed, in which *in situ* generated **2** was reacted with styrene to potentially form the anionic alkyl species  $[(^t\text{BuPCP})\text{Ir}(\text{phenylethyl})]^-$ . Experimental results do not show a molecular ion peak in accordance with  $[(^t\text{BuPCP})\text{Ir}(\text{phenylethyl})]^-$ ; thus, we conclude that despite thermodynamic feasibility for  $\text{CO}_2$  insertion into the Ir–H bond of **2**, styrene does not react analogously as a dominant pathway, potentially because of steric hindrance of the larger substrate.

Additional NMR control reactions, in which Ir(III) complex **1** was reacted with one equivalent of styrene and  $\text{H}_2\text{O}$  in  $\text{THF-d}_8$  yielded no detectable ethyl benzene or an identifiable iridium alkyl complex (SI, Figures S11 and S12); thus, excluding this complex as the active species during the catalytic cycle.

Importantly, the combined results on the reactivity of **1** suggest a so far unique electro-hydrogenation cycle that is driven by (formal) oxidative addition of  $\text{H}_2\text{O}$  rather than by the common path of  $\text{H}^+$  reduction from a Brønsted acid. If the reactive hydride species are indeed regenerated by  $\text{H}_2\text{O}$  activation rather than by  $\text{H}^+$  reduction, the catalytic current in CV experiments should be independent of proton activity. In line with this assumption, CV control experiments in which KOH was added to the electrolyte solution under catalytic conditions, to drastically reduce the activity of  $\text{H}^+$ , did show little to no effect on the catalytic current response (Figure 4). Even though the pH value is not a well-defined concept in organic solvents with small amounts of water, addition of KOH as a strong Brønsted

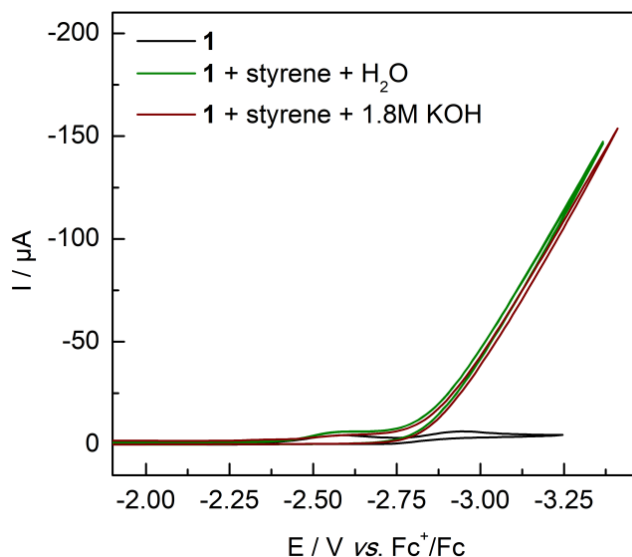


**Figure 4.** CV of **1** (3 mg) in THF with 0.1 M  $\text{Bu}_4\text{NPF}_6$  recorded at a scan rate of 0.2 V/s using a GC disc (1 mm) working electrode, a Pt wire counter electrode, and a silver wire pseudo reference electrode. The black trace shows complex **1** without substrates, the green trace shows the catalytic current originating in the presence of  $\text{H}_2\text{O}$  and styrene, the brown trace shows the catalytic current response when KOH is added to the electrolyte to reduce proton activity.

base severely reduces  $\text{H}^+$  activity in the electrolyte, while the activity of  $\text{H}_2\text{O}$  molecules remains high, independent of KOH addition. Accordingly, the control experiment presented in Figure 4 suggest a reaction mechanism for electro-hydrogenation with **1** that is indeed mediated by  $\text{H}_2\text{O}$  activation rather than by  $\text{H}^+$  reduction, as proposed in Scheme 2.

This is contrasting the previously reported reaction mechanism for  $\text{CO}_2$  reduction to formate by iridium pincer complexes in acetonitrile as proposed by Brookhart and coworkers. In their case, a *cationic* Ir(III) hydride is reported as the electro reactive species, which undergoes a concerted two-electron reduction to Ir(I) at a mild reduction potential of  $-1.4$  V vs. NHE (corresponding to *ca.*  $-2.0$  V vs.  $\text{Fc}^+/\text{Fc}$ ).<sup>50</sup> The electro-generated Ir(I) was then reported to react with  $\text{H}^+$  from water as a simple proton source to generate an Ir(III) di-hydride as the hydrogenating species for  $\text{CO}_2$  reduction.<sup>41</sup>

Instead, the herein reported example of electrocatalytic alkene hydrogenation uses  $\text{H}_2\text{O}$  as H-donor in the sense of transfer hydrogenation. Reactive metal hydrides driving the catalytic hydrogenation are formed *via* intramolecular activation of the coordinated H-donor water, instead of by simple proton reduction. This renders the reported model system distinctly different from the majority of electro-hydrogenation examples reported in the literature, which rely on stoichiometric use of protons from Brønsted acids and thus, low pH electrolyte. Building on this finding, electrocatalytic transfer hydrogenation (e-TH) with water is an auspicious concept to be explored in more detail in the

future. Despite the potential to enable electrohydrogenation of substrates that cannot tolerate acidic media, it should be emphasized that electrohydrogenation at the working electrode requires water oxidation at the counter electrode as the second half reaction. As known from the Pourbaix diagram, H<sub>2</sub>O oxidation is easier at high pH; thus, e-TH with water molecules instead of H<sup>+</sup> paves the way to operate electrolysis at drastically reduced cell potentials, given that water oxidation potentials are reduced by ~ 830 mV when switching from pH = 0 to pH = 14 electrolytes.<sup>51</sup> Acknowledging that both necessary overpotentials of e-TH half reaction and H<sub>2</sub>O oxidation contribute to the cell potential, it is clear that catalyst **1** can merely serve as a model towards energy efficient e-TH. For actually energy efficient processes, hydrogenation overpotentials must be drastically reduced by catalyst design in the future.

## CONCLUSIONS

In summary, the electrochemical reactivity of the Ir(III) complex [(<sup>t</sup>BuPCP)Ir(H)(Cl)] (**1**) was investigated in THF electrolyte, which revealed the formation of anionic Ir(I) hydride complex [(<sup>t</sup>BuPCP)Ir(H)]<sup>−</sup> (**2**) upon electrochemical reduction at −2.84 V vs. Fc<sup>+</sup>/Fc. The existence of **2**, previously only postulated based on quantum chemical calculations, was now confirmed by LIFDI-MS experiments with *in situ* reduced samples of **1**. Cyclic voltammetry experiments revealed that **2** mediates electrocatalytic transfer hydrogenation (e-TH) of styrene as a model substrate with pH neutral H<sub>2</sub>O as the H-donor and electrons provided by a glassy carbon working electrode as external reducing agent. Chronoamperometry experiments confirmed a high faradaic efficiency of 96% for the conversion of styrene to ethylbenzene as the only product according to <sup>1</sup>H NMR, with a turnover frequency of 1670 h<sup>−1</sup> at an electrolysis potential of −3.1 V. Control experiments in which KOH was added to the electrolyte, in order to reduce the activity of H<sup>+</sup> during electro hydrogenation, yielded the same catalytic current as the addition of pure water. This result strongly suggests that the newly found e-TH reactivity of **1** as presented herein, is independent of protons and mediated by oxidative addition of H<sub>2</sub>O to Ir(I) for generation of reactive iridium hydride species. As such, this H<sup>+</sup> independent example of e-TH may inspire pathways to generally enable H<sub>2</sub>O as sustainable and abundant H-donor in the broad context of transfer hydrogenation. For electrocatalytic reaction design in general, the H<sup>+</sup> independency of e-TH with water will allow to optimize conditions of the reaction medium (electrolyte) for substrate compatibility and to support the OER at the counter electrode, without compromising catalytic performance at the working electrode.

## ASSOCIATED CONTENT

**Supporting Information.** The Supporting Information contains experimental details, synthesis procedures, relevant

NMR data, additional electrochemical experiments and LIFDI-MS details.

## AUTHOR INFORMATION

### Corresponding Author

\* Dominik P. Halter

Email: [Dominik.Halter@tum.de](mailto:Dominik.Halter@tum.de)

Department of Chemistry, Technical University of Munich, Lichtenbergstraße 4, 85787 Garching, Germany.

ORCID: 0000-0003-0733-8955

### Patrick Mollik

Department of Chemistry, Technical University of Munich, Lichtenbergstraße 4, 85787 Garching, Germany.

ORCID: 0000-0001-6657-6633

### Alexander M. Frantz

Department of Chemistry, Technical University of Munich, Lichtenbergstraße 4, 85787 Garching, Germany.

ORCID: 0000-0001-8674-2985

## Notes

The authors declare no competing financial interest.

## ACKNOWLEDGMENT

D.H. thanks the Fonds der Chemischen Industrie for a Liebig Fellowship. This work was further supported by a Feodor Lynen Return Fellowship for D.H. by the Alexander von Humboldt Foundation and the TUM Junior Fellow Funds by the Technical University of Munich. Richard Zell is acknowledged for support with headspace analysis by gas chromatography. P.M., A.F. and D.H. are grateful for support from Roland A. Fischer and his chair of Inorganic and Metal-Organic Chemistry at TUM.

## REFERENCES

- (1) Alig, L.; Fritz, M.; Schneider, S. First-Row Transition Metal (De)Hydrogenation Catalysis Based On Functional Pincer Ligands. *Chem. Rev.* **2019**, *119*, 2681–2751.
- (2) Stoffels, M. A.; Klauck, F. J. R.; Hamadi, T.; Glorius, F.; Leker, J. Technology Trends of Catalysts in Hydrogenation Reactions: A Patent Landscape Analysis. *Adv. Synth. Catal.* **2020**, *362*, 1258–1274.
- (3) Blaser, H.-U.; Malan, C.; Pugin, B.; Spindler, F.; Steiner, H.; Studer, M. Selective Hydrogenation for Fine Chemicals: Recent Trends and New Developments. *Adv. Synth. Catal.* **2003**, *345*, 103–151.
- (4) Jorschick, H.; Vogl, M.; Preuster, P.; Bösmann, A.; Wasserscheid, P. Hydrogenation of liquid organic hydrogen carrier systems using multicomponent gas mixtures. *Int. J. Hydrog. Energy* **2019**, *44*, 31172–31182.
- (5) Nakagawa, Y.; Tamura, M.; Tomishige, K. Catalytic Reduction of Biomass-Derived Furanic Compounds with Hydrogen. *ACS Catal.* **2013**, *3*, 2655–2668.
- (6) Werkmeister, S.; Neumann, J.; Junge, K.; Beller, M. Pincer-Type Complexes for Catalytic (De)Hydrogenation and

Transfer (De)Hydrogenation Reactions: Recent Progress. *Chem. Eur. J.* **2015**, *21*, 12226–12250.

(7) Vries, J. G. d.; Elsevier, C. J., Eds. *The handbook of homogeneous hydrogenation*; Wiley-VCH, 2007.

(8) Wang, D.; Astruc, D. The golden age of transfer hydrogenation. *Chem. Rev.* **2015**, *115*, 6621–6686.

(9) Nie, R.; Tao, Y.; Nie, Y.; Lu, T.; Wang, J.; Zhang, Y.; Lu, X.; Xu, C. C. Recent Advances in Catalytic Transfer Hydrogenation with Formic Acid over Heterogeneous Transition Metal Catalysts. *ACS Catal.* **2021**, *11*, 1071–1095.

(10) Hu, X.; Wang, G.; Qin, C.; Xie, X.; Zhang, C.; Xu, W.; Liu, Y. Ligandless nickel-catalyzed transfer hydrogenation of alkenes and alkynes using water as the hydrogen donor. *Org. Chem. Front.* **2019**, *6*, 2619–2623.

(11) Gao, Y.; Zhang, X.; Laishram, R. D.; Chen, J.; Li, K.; Zhang, K.; Zeng, G.; Fan, B. Cobalt-Catalyzed Transfer Hydrogenation of  $\alpha$ -Ketoesters and N-Cyclicsulfonylimides Using  $H_2O$  as Hydrogen Source. *Adv. Synth. Catal.* **2019**, *361*, 3991–3997.

(12) Li, K.; Khan, R.; Zhang, X.; Gao, Y.; Zhou, Y.; Tan, H.; Chen, J.; Fan, B. Cobalt catalyzed stereodivergent semihydrogenation of alkynes using  $H_2O$  as the hydrogen source. *Chem. Commun.* **2019**, *55*, 5663–5666.

(13) Guo, S.; Wang, X.; Zhou, J. S. Asymmetric Umpolung Hydrogenation and Deuteration of Alkenes Catalyzed by Nickel. *Org. Lett.* **2020**, *22*, 1204–1207.

(14) Rao, S.; Prabhu, K. R. Stereodivergent Alkyne Reduction by using Water as the Hydrogen Source. *Chem. Eur. J.* **2018**, *24*, 13954–13962.

(15) Xuan, Q.; Song, Q. Diboron-Assisted Palladium-Catalyzed Transfer Hydrogenation of N-Heteroaromatics with Water as Hydrogen Donor and Solvent. *Org. Lett.* **2016**, *18*, 4250–4253.

(16) Derosa, J.; Garrido-Barros, P.; Peters, J. C. Electrocatalytic Reduction of C-C  $\pi$ -Bonds via a Cobaltocene-Derived Concerted Proton-Electron Transfer Mediator: Fumarate Hydrogenation as a Model Study. *J. Am. Chem. Soc.* **2021**, *143*, 9303–9307.

(17) Li, J.; He, L.; Liu, X.; Cheng, X.; Li, G. Electrochemical Hydrogenation with Gaseous Ammonia. *Angew. Chem. Int. Ed.* **2019**, *58*, 1759–1763.

(18) Bu, J.; Liu, Z.; Ma, W.; Zhang, L.; Wang, T.; Zhang, H.; Zhang, Q.; Feng, X.; Zhang, J. Selective electrocatalytic semihydrogenation of acetylene impurities for the production of polymer-grade ethylene. *Nat. Catal.* **2021**, *4*, 557–564.

(19) Li, B.; Ge, H. Highly selective electrochemical hydrogenation of alkynes: Rapid construction of mechanochromic materials. *Sci. Adv.* **2019**, *5*, eaaw2774.

(20) Langer, S. H.; Yurchak, S. Electrochemical Reduction of the Benzene Ring by Electrogenative Hydrogenation. *J. Electrochem. Soc.* **1969**, *116*, 1228.

(21) Inami, Y.; Ogihara, H.; Nagamatsu, S.; Asakura, K.; Yamanaka, I. Synergy of Ru and Ir in the Electrohydrogenation of Toluene to Methylcyclohexane on a Ketjenblack-

Supported Ru-Ir Alloy Cathode. *ACS Catal.* **2019**, *9*, 2448–2457.

(22) Itoh, N.; Xu, W.; Hara, S.; Sakaki, K. Electrochemical coupling of benzene hydrogenation and water electrolysis. *Catal. Today* **2000**, *56*, 307–314.

(23) Peters, B. K.; Rodriguez, K. X.; Reisberg, S. H.; Beil, S. B.; Hickey, D. P.; Kawamata, Y.; Collins, M.; Starr, J.; Chen, L.; Udyavara, S.; Klunder, K.; Gorey, T. J.; Anderson, S. L.; Neuhoff, M.; Minter, S. D.; Baran, P. S. Scalable and safe synthetic organic electroreduction inspired by Li-ion battery chemistry. *Science* **2019**, *363*, 838–845.

(24) Fokin, I.; Siewert, I. Chemoselective Electrochemical Hydrogenation of Ketones and Aldehydes with a Well-Defined Base-Metal Catalyst. *Chem. Eur. J.* **2020**, *26*, 14137–14143.

(25) Chalkley, M. J.; Garrido-Barros, P.; Peters, J. C. A molecular mediator for reductive concerted proton-electron transfers via electrocatalysis. *Science* **2020**, *369*, 850–854.

(26) Lam, C. H.; Lowe, C. B.; Li, Z.; Longe, K. N.; Rayburn, J. T.; Caldwell, M. A.; Houdek, C. E.; Maguire, J. B.; Saffron, C. M.; Miller, D. J.; Jackson, J. E. Electrocatalytic upgrading of model lignin monomers with earth abundant metal electrodes. *Green Chem.* **2015**, *17*, 601–609.

(27) Kim, S.; Kwon, E. E.; Kim, Y. T.; Jung, S.; Kim, H. J.; Huber, G. W.; Lee, J. Recent advances in hydrodeoxygenation of biomass-derived oxygenates over heterogeneous catalysts. *Green Chem.* **2019**, *21*, 3715–3743.

(28) Liu, W.; You, W.; Gong, Y.; Deng, Y. High-efficiency electrochemical hydrodeoxygenation of bio-phenols to hydrocarbon fuels by a superacid-noble metal particle dual-catalyst system. *Energy Environ. Sci.* **2020**, *13*, 917–927.

(29) Kurimoto, A.; Sherbo, R. S.; Cao, Y.; Loo, N. W. X.; Berlinguette, C. P. Electrolytic deuteration of unsaturated bonds without using  $D_2$ . *Nat. Catal.* **2020**, *3*, 719–726.

(30) Yang, J.; Qin, H.; Yan, K.; Cheng, X.; Wen, J. Advances in Electrochemical Hydrogenation Since 2010. *Adv. Synth. Catal.* **2021**, *363*, 5407–5416.

(31) Sherbo, R. S.; Delima, R. S.; Chiykowski, V. A.; MacLeod, B. P.; Berlinguette, C. P. Complete electron economy by pairing electrolysis with hydrogenation. *Nat. Catal.* **2018**, *1*, 501–507.

(32) Akhade, S. A.; Singh, N.; Gutiérrez, O. Y.; Lopez-Ruiz, J.; Wang, H.; Holladay, J. D.; Liu, Y.; Karkamkar, A.; Weber, R. S.; Padmaperuma, A. B.; Lee, M.-S.; Whyatt, G. A.; Elliott, M.; Holladay, J. E.; Male, J. L.; Lercher, J. A.; Rousseau, R.; Glezakou, V.-A. Electrocatalytic Hydrogenation of Biomass-Derived Organics: A Review. *Chem. Rev.* **2020**, *120*, 11370–11419.

(33) Wakisaka, M.; Kunitake, M. Direct electrochemical hydrogenation of toluene at Pt electrodes in a microemulsion electrolyte solution. *Electrochem. Commun.* **2016**, *64*, 5–8.

(34) Carrero, H.; Gao, J.; Rusling, J. F.; Lee, C.-W.; Fry, A. J. Direct and catalyzed electrochemical syntheses in microemulsions. *Electrochim. Acta* **1999**, *45*, 503–512.

- (35) Li, P.; Zhao, R.; Chen, H.; Wang, H.; Wei, P.; Huang, H.; Liu, Q.; Li, T.; Shi, X.; Zhang, Y.; Liu, M.; Sun, X. Recent Advances in the Development of Water Oxidation Electrocatalysts at Mild pH. *Small* **2019**, *15*, 1805103.
- (36) Ozerov, O. V. Oxidative addition of water to transition metal complexes. *Chem. Soc. Rev.* **2009**, *38*, 83–88.
- (37) Moulton, C. J.; Shaw, B. L. Transition metal–carbon bonds. Part XLII. Complexes of nickel, palladium, platinum, rhodium and iridium with the tridentate ligand 2,6-bis[(di-*t*-butylphosphino)methyl]phenyl. *J. Chem. Soc., Dalton Trans.* **1976**, 1020–1024.
- (38) Rimoldi, M.; Mezzetti, A. Silica-grafted 16-electron hydride pincer complexes of iridium(III) and their soluble analogues: synthesis and reactivity with CO. *Inorg. Chem.* **2014**, *53*, 11974–11984.
- (39) Wang, D. Y.; Choliy, Y.; Haibach, M. C.; Hartwig, J. F.; Krogh-Jespersen, K.; Goldman, A. S. Assessment of the Electronic Factors Determining the Thermodynamics of "Oxidative Addition" of C–H and N–H Bonds to Ir(I) Complexes. *J. Am. Chem. Soc.* **2016**, *138*, 149–163.
- (40) Osadchuk, I.; Tamm, T.; Ahlquist, M. S. G. Reduced State of Iridium PCP Pincer Complexes in Electrochemical CO<sub>2</sub> Hydrogenation. *ACS Catal.* **2016**, *6*, 3834–3839.
- (41) Kang, P.; Cheng, C.; Chen, Z.; Schauer, C. K.; Meyer, T. J.; Brookhart, M. Selective electrocatalytic reduction of CO<sub>2</sub> to formate by water-stable iridium dihydride pincer complexes. *J. Am. Chem. Soc.* **2012**, *134*, 5500–5503.
- (42) Dye, J. L. Electrides: ionic salts with electrons as the anions. *Science* **1990**, *247*, 663–668.
- (43) Morales-Morales, D.; Lee, D. W.; Wang, Z.; Jensen, C. M. Oxidative Addition of Water by an Iridium PCP Pincer Complex: Catalytic Dehydrogenation of Alkanes by IrH(OH){C<sub>6</sub>H<sub>3</sub>-2,6-(CH<sub>2</sub>PBu<sup>*t*</sup>)<sub>2</sub>}. *Organometallics* **2001**, *20*, 1144–1147.
- (44) Kanzelberger, M.; Singh, B.; Czerw, M.; Krogh-Jespersen, K.; Goldman, A. S. Addition of C–H Bonds to the Catalytically Active Complex (PCP)Ir (PCP =  $\eta^3$ -2,6-(<sup>*t*</sup>Bu<sub>2</sub>PCH<sub>2</sub>)<sub>2</sub>C<sub>6</sub>H<sub>3</sub>). *J. Am. Chem. Soc.* **2000**, *122*, 11017–11018.
- (45) Johnson, S. I.; Nielsen, R. J.; Goddard, W. A. Selectivity for HCO<sub>2</sub><sup>–</sup> over H<sub>2</sub> in the Electrochemical Catalytic Reduction of CO<sub>2</sub> by (POCOP)IrH<sub>2</sub>. *ACS Catal.* **2016**, *6*, 6362–6371.
- (46) Cao, L.; Sun, C.; Sun, N.; Meng, L.; Chen, D. Theoretical mechanism studies on the electrocatalytic reduction of CO<sub>2</sub> to formate by water-stable iridium dihydride pincer complex. *Dalton Trans.* **2013**, 42, 5755–5763.
- (47) Abura, T.; Ogo, S.; Watanabe, Y.; Fukuzumi, S. Isolation and crystal structure of a water-soluble iridium hydride: a robust and highly active catalyst for acid-catalyzed transfer hydrogenations of carbonyl compounds in acidic media. *J. Am. Chem. Soc.* **2003**, *125*, 4149–4154.
- (48) Goes, S. L.; Mayer, M. N.; Nutting, J. E.; Hooper-Burkhardt, L. E.; Stahl, S. S.; Rafiee, M. Deriving the Turnover Frequency of Aminoxyl-Catalyzed Alcohol Oxidation by Chronoamperometry: An Introduction to Organic Electrocatalysis. *J. Chem. Educ.* **2021**, *98*, 600–606.
- (49) Connor, G. P.; Lease, N.; Casuras, A.; Goldman, A. S.; Holland, P. L.; Mayer, J. M. Protonation and electrochemical reduction of rhodium- and iridium-dinitrogen complexes in organic solution. *Dalton Trans.* **2017**, 46, 14325–14330.
- (50) Pavlishchuk, V. V.; Addison, A. W. Conversion constants for redox potentials measured versus different reference electrodes in acetonitrile solutions at 25°C. *Inorg. Chim. Acta* **2000**, *298*, 97–102.
- (51) Kanan, M. W.; Nocera, D. G. In Situ Formation of an Oxygen-Evolving Catalyst in Neutral Water Containing Phosphate and Co<sup>2+</sup>. *Science* **2008**, *321*, 1072–1075.